

Supporting Information

High-Voltage Lithium-Metal Battery Enabled by Ethylene Glycol Bis(Propionitrile)
Ether-LiNO₃ Synergetic Additives

Shaopeng Li^{a,b}, *Kangsheng Huang*^a, *Langyuan Wu*^a, *Dewei Xiao*^a, *Jiang Long*^a,
Chenhui Wang^a, *Hui Dou*^a, *Pu Chen*^{*b} and *Xiaogang Zhang*^{*a}

^a Jiangsu Key Laboratory of Electrochemical Energy Storage Technologies, College of Materials Science and Technology, Nanjing University of Aeronautics and Astronautics, Nanjing, 210016, P. R. China.

^b Department of Chemical Engineering and Waterloo Institute of Nanotechnology, University of Waterloo, N2L 3G1, Canada.

1. Experimental Section

4.1. Electrolyte Preparation

DENE was obtained from Fujian Chuangxin Science and Develops Corporation. and was dried with 4 Å molecular sieves before use. 1M LiPF₆ in EC/DMC (1:1 by vol) with 5% FEC and LiNO₃ (>99.9%) were purchased from Shanshan Advanced Materials Corporation. The DENE/LiNO₃ additive was homemade by dissolving 1M LiNO₃ into DENE with 60°C heating. The DLE electrolytes were prepared simply by adding different contents of DENE/LiNO₃ (1M) additive into 1M LiPF₆ in EC/DMC (1:1 by vol) with 5% FEC and stirring at 25°C.

4.2. Battery Fabrication and Electrochemical Measurements

LiCoO₂ (LCO) cathode electrode laminates (active material loading is about 12.0 mg cm⁻²) were homemade mixing by 90 wt% LCO, 5 wt% acetylene black, 5 wt % PVDF with moderate amount of NMP. The electrode was cut into discs (10 mm in diameter) and dried at 100 °C under vacuum overnight. Lithium chips (100 μm thick) were purchased from Tianjin Zhong Neng Corporation. Coin cell assembly was carried out in an argon-filled glovebox by using the 2016 type. The electrolyte volume in a coin cell was 60 μl and utilized a single piece of Celgard 2500 separator. A Land Instruments Battery Tester was used for the cycling performance measurements. The linear sweep voltammetry (LSV), cyclic voltammetry (CV) and electrochemical impedance spectroscopy (EIS) were tested on a Biologic electrochemical workstation. LSV curves were tested with a scanning rate of 10 mV s⁻¹ from 2.5V to 6 V at room temperature. (EIS) was performed with a frequency range of 1×10⁵–1×10⁻² Hz and a disturbance amplitude of 5 mV. The Li plating/stripping Coulombic efficiency (CE) was calculated as reported before[1]. The calculation formula of CE is:

$$CE = \frac{nQ_C + Q_S}{nQ_C + Q_T} \quad (1)$$

Q_T: a given amount of pre-deposition Li.

Q_C: capacity during the cycle.

n: the cycle number

Q_S: The final stripping amount of Li.

4.3. Materials Characterization

In situ optical observation: The in-situ optical observation unit is supported by the Beijing Scistar Technology Co. Ltd, using lithium foil as working electrodes and counter electrodes. The two electrodes were aligned in parallel with a gap. The in-situ observation of the Li depositing process was conducted with an optical microscope and ChenHua CHI760 system.

In situ electrochemical dilatometry measurement: ECD-3-Nano (EL-CELL, Germany) was used to record the thickness change of lithium metal during plating/stripping in real time. The cell was assembled with the working electrode (10 mm in diameter), a Li metal counter electrode and a borosilicate glass with 0.5 mL of the same electrolyte as in the coin cells. The chronopotentiometry measurement was tested between -5V and 5 V at the current density of 1 mA cm⁻² in a chamber with a constant temperature of 25 °C.

In operando DEMS spectroscopy: The DEMS system was built with a Pfeiffer Vacuum QMA410 system and a Swagelok type DEMS cell with two PEEK capillary tubes as purge gas inlet and outlet. The flow rate of purge gas was controlled by a digital mass flow meter (Bronkhorst). 3 mL min⁻¹ of high purity Ar was used as a carrier gas and acted as the internal tracer gas with known invariable flux. A cold trap cooled by carbon dioxide ice was used to avoid the volatilization of electrolyte components.

Li metal anodes and LiCoO₂ cathodes after predesigned cycles were cleaned with DMC to wipe off the remaining lithium salts and electrolytes. Finally, the electrode was dried in a vacuum environment for SEM analysis and TOF-SIMS tests (LYRA3 TESCAN), ex situ X-ray photoelectron spectroscopy (XPS) profiles (Thermo Fisher Scientific ESCALAB 250Xi System).

The contents of Co ions dissolved in electrolytes were measured by an inductively coupled plasma-atomic emission spectrometer (ICP-AES, Agilent 7700). The cycled electrolytes were washed by DMC and dissolved in 10 mL 2% HNO₃.

4.4. Simulation parameters.

In this Molecular dynamics (MD) simulation system, the x, y and Z dimensions were periodic boundary conditions. The OPLS force field, which is suitable for the electrolyte solution, was used to optimize sample structures for preliminary structural optimization. Atomic charges of ions were multiplied by a scale factor of 0.73 to correct the polarization effect of anion and cation. First, the conjugate gradient algorithm and energy minimization were performed to obtain a stable structure before using dynamic simulations. Each sample was then equilibrated under the NPT ensemble at a constant temperature of 400 K to achieve an equilibrium state with zero pressure for 5 ns. Subsequently, the system temperature was reduced from 400 K to 298 K for annealing 5 ns under the NPT ensemble (under 1 atmosphere). The Andersen feedback thermostat and Berendsen barostat algorithm were applied in the system with temperature and pressure conversion. Next, MD simulations were further carried out for 10 ns with a time step of 1 fs per integration step under the ensemble conditions of NVT (298 K). System energy can be obtained through structural optimization using energy minimization. The radial distribution functions (RDFs), $g(r)$, give the probability of molecules occurring at a distance (r).

The first principles calculations were performed by using the Quantum Espresso [2, 3]. The projector-augmented-wave (PAW) [4] generalized gradient approximations (GGA) of Perdew-Burke-Ernzerhof (PBE) [5] pseudopotentials were adopted for the exchange-correlation functional. DFT+U method was applied to treat the strongly correlated cobalt 3d orbital electrons with effective U value of 3.3 eV. A cutoff energy of 500eV was set to ensure the precision of the calculations. The Gamma centered $1 \times 1 \times 1$ k-point set was chosen. We introduced a vacuum spacing of 25 Å in the z-axis direction to avoid the interaction between periodic images. The convergence criterions were 10^{-4} eV and $0.05 \text{ eV} / \text{Å}$ for electron energy and ions force respectively in all calculations. The 3D crystal structures for the equilibrium structures were visualized by the VESTA [6] code.

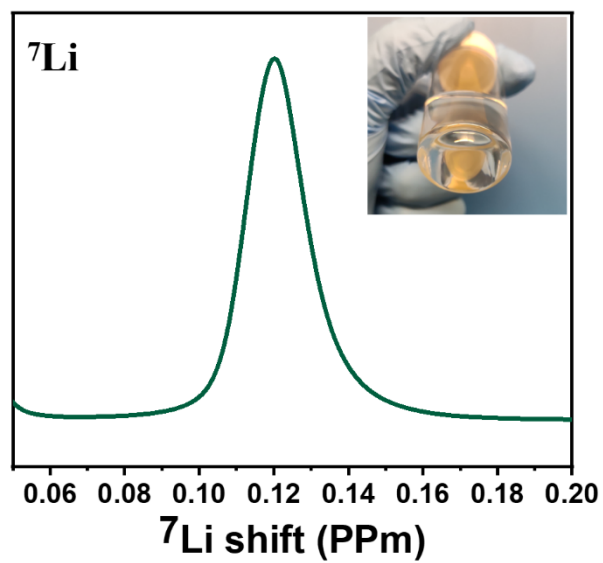


Figure S1. ${}^7\text{Li}$ NMR spectra of DENE/LiNO₃ (1 M) composite additive(extracted with CDCl₃ solvent), the inset is an optical image of DENE/LiNO₃ (1 M) composite.

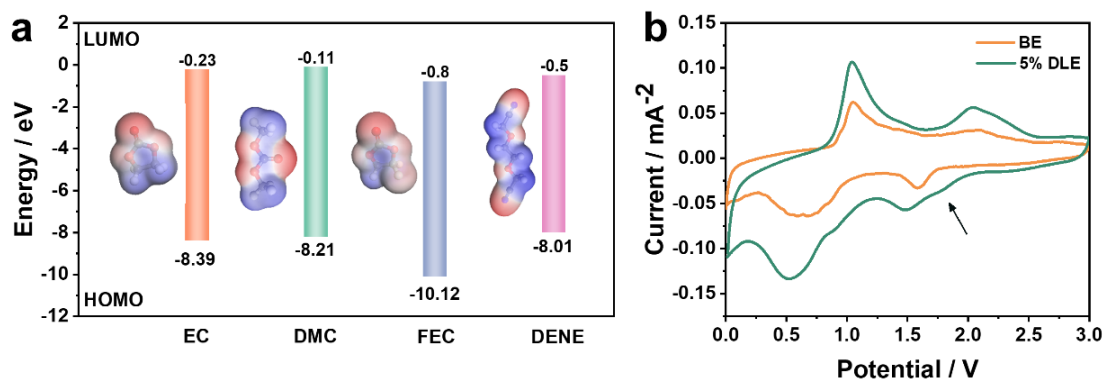


Figure S2. a) The electrostatic potential and HOMO/LUMO energy levels of DENE and other solvents. b) Cyclic voltammetry measurement from 0 to 3 V.

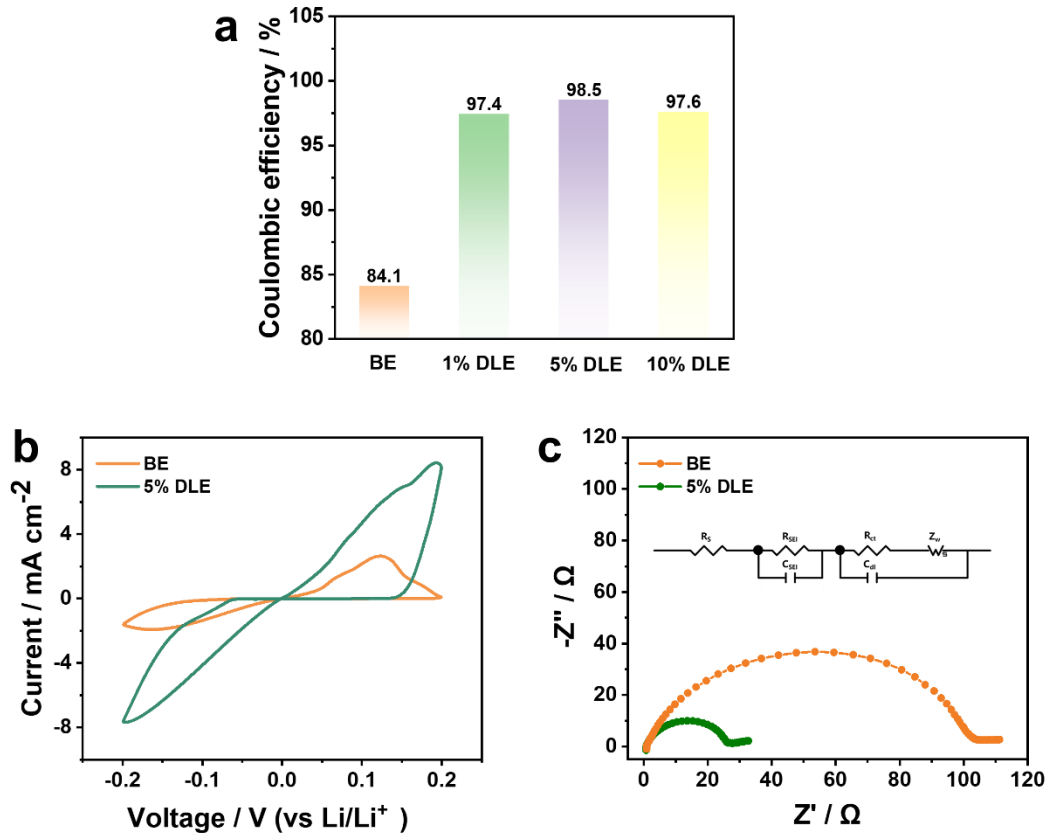


Figure S3. a) CE in the base electrolyte and DLE electrolytes at 0.5 mA cm^{-2} and 1 mAh cm^{-2} . b) CV scans of Li plating/stripping in the base electrolyte and 5% DLE at a scanning speed of 0.2 mV s^{-1} . c) Nyquist plots of the Li||Li symmetric cells after 100 cycle at 1 mA cm^{-2} and 1 mAh cm^{-2}

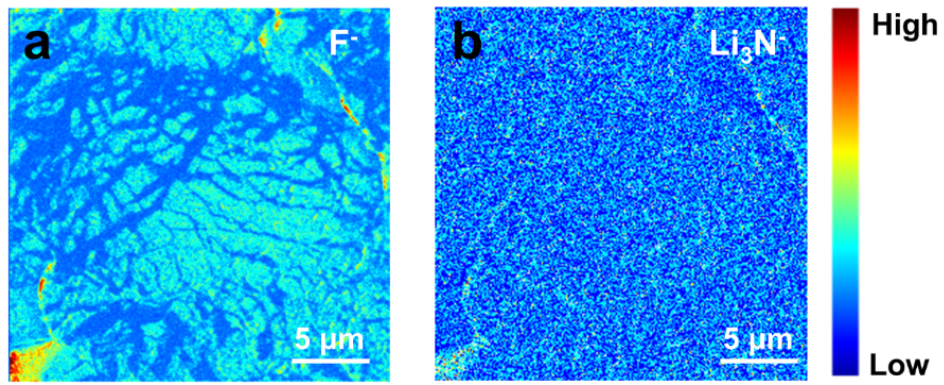


Figure S4. a) F⁻, b) Li₃N⁻ high lateral resolution secondary ion maps of Li anode after depth sputtering.

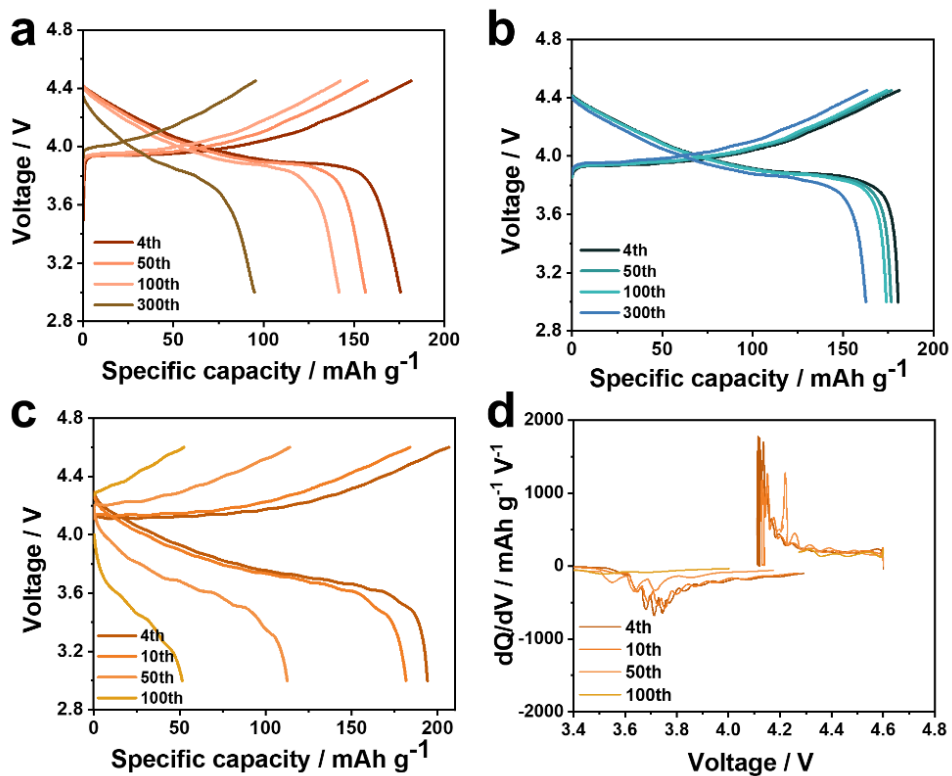


Figure S5. The selected charge/discharge profiles of Li||LCO between 3.0 and 4.45 V in a) base electrolyte, b) 5% DLE. c) The selected charge/discharge profiles of Li||LCO between 3.0 and 4.6 V in base electrolyte (d) Corresponding dQ/dV curves at the selected cycles in base electrolyte.

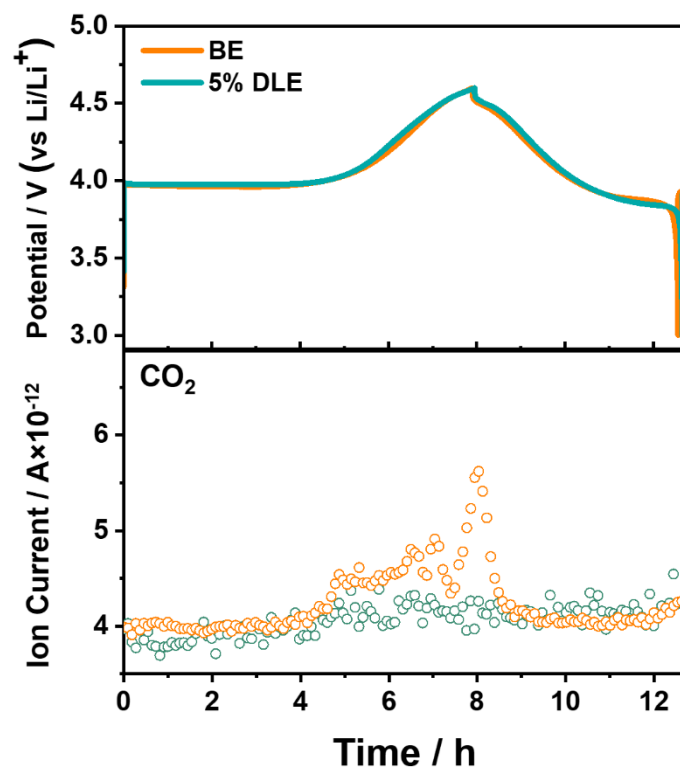


Figure S6. Gas evolution from base electrolyte (origin line) and 5% DLE (green line) in Li||LCO cell at 0.1C and room temperature.

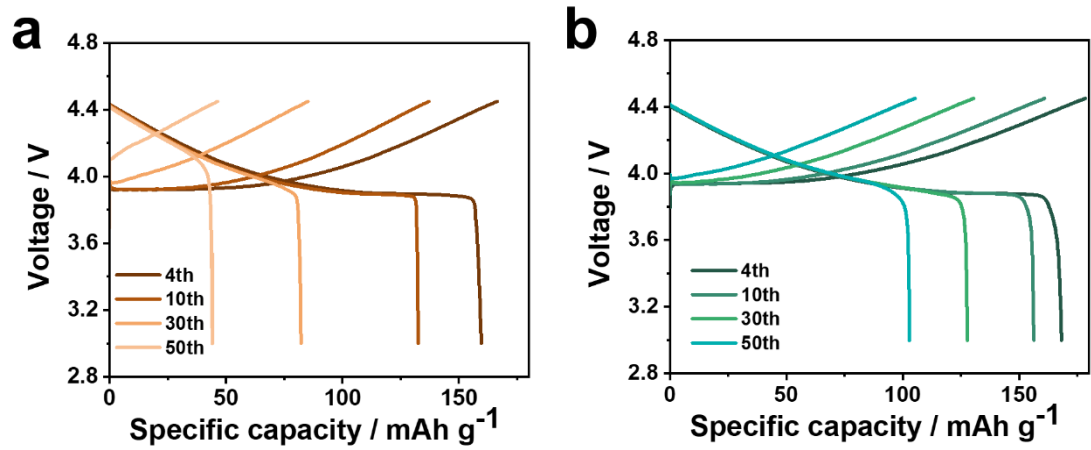


Figure S7. The selected charge/discharge profiles of Cu||LCO anode-free cell in a) base electrolyte b) 5% DLE

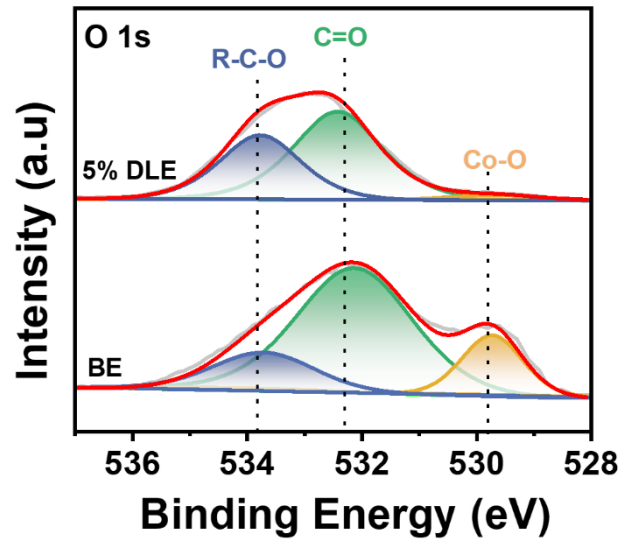


Figure S8. O 1s XPS spectra of LCO cathodes after 100 cycles

Table S1. The detailed fitted values of electrochemical impedance spectroscopy for

Li||Li cells in different electrolytes after 100 cycles.

Electrolyte	R_s/Ω	R_{SEI}/Ω	R_{CT}/Ω
BE	1.57	94.76	13.08
5% DLE	0.87	25.73	8.01

Table S2 Variation of lithium metal thickness during plating/stripping

Electrolyte	Cycle	l_1 (μm)	l_2 (μm)	$\Delta\mu$ (μm)	α ($\mu\text{m cm}^2/\text{mAh}$)
BE	1 st	3.88	0.48	0.48	3.88
	2 nd	6.95	3.64	3.64	6.47
	3 rd	16.09	10.98	10.98	12.45
5% DLE	1 st	2.89	0.10	0.10	2.89
	2 nd	3.67	0.20	0.20	3.57
	3 rd	4.78	0.99	0.99	4.58

References

- [1] B. D. Adams, J. M. Zheng, X. D. Ren, W. Xu, J. G. Zhang, Accurate Determination of Coulombic Efficiency for Lithium Metal Anodes and Lithium Metal Batteries, *Adv Energy Mater.* 8 (2018) 1702097
- [2] G. Kresse, J. Furthmüller, Efficient iterative schemes for ab initio total-energy calculations using a plane-wave basis set, *Phys. Rev. B*, 54 (1996) 11169.
- [3] G. Kresse, D. Joubert, From ultrasoft pseudopotentials to the projector augmented-wave method, *Phys. Rev. B*, 59 (1999) 1758.
- [4] P.E. Blöchl, Projector augmented-wave method, *Phys. Rev. B*, 50 (1994) 17953.
- [5] J.P. Perdew, K. Burke, M. Ernzerhof, Generalized gradient approximation made simple, *Phys. Rev. Lett.*, 77 (1996) 3865.
- [6] K. Momma, F. Izumi, VESTA: a three-dimensional visualization system for electronic and structural analysis, *J. Appl. Crystallogr.*, 41 (2008) 653-658.